PHYSICAL REVIEW A **78**, 061601(R) (2008)

Association of ultracold double-species bosonic molecules

C. Weber,[1,3] G. Barontini,[1] J. Catani,[1,2] G. Thalhammer,[1] M. Inguscio,[1,2] and F. Minardi[1,2]
[1]*LENS, European Laboratory for Non-Linear Spectroscopy and Dipartimento di Fisica, Università di Firenze, via N. Carrara 1, I-50019 Sesto Fiorentino, Firenze, Italy*
[2]*CNR-INFM, via G. Sansone 1, I-50019 Sesto Fiorentino, Firenze, Italy*
[3]*Institut für Angewandte Physik, Universität Bonn, Wegelerstraße 8, D-53115 Bonn, Germany*
(Received 29 August 2008; revised manuscript received 15 October 2008; published 3 December 2008)

We report on the creation of heterospecies bosonic molecules, associated from an ultracold Bose-Bose mixture of ^{41}K and ^{87}Rb, by using a resonantly modulated magnetic field close to two Feshbach resonances. We measure the binding energy of the weakly bound molecular states versus the Feshbach field and compare our results to theoretical predictions. We observe the broadening and asymmetry of the association spectrum due to the thermal distribution of the atoms and a frequency shift occurring when the binding energy depends nonlinearly on the Feshbach field. A simple model is developed to quantitatively describe the association process. This work represents a required step toward Bose-Einstein condensates of dipolar molecules.

DOI: 10.1103/PhysRevA.78.061601 PACS number(s): 67.85.−d, 34.20.Cf, 34.50.−s

Ultracold polar molecules promise to open an avenue in the domain of quantum degenerate gases and precision measurements. Degenerate molecules are sought primarily to produce a gas with strong long-range interactions, stemming from the coupling of electric-dipole moments that heterospecies dimers feature. Such molecules would create strongly correlated systems with a wealth of quantum phases [1], provide candidate qubits [2,3], allow for the next generation of dipolar Bose-Einstein condensates (BECs) [4], and help in the search for the electron dipole moment [5]. Starting from ultracold atoms, molecules have been successfully created following two different approaches: photoassociation [6] and magnetoassociation [7], but few experiments have hitherto reported the production of Feshbach heteronuclear dimers. Three groups have reported the creation of fermionic KRb molecules [8–10], while the only bosonic dimer so far associated is ^{85}Rb^{87}Rb [11], which can have only a very small permanent electric dipole since the constituents share the same electronic configuration. Heterospecies bosonic dimers—i.e., the constituents of the dipolar BEC envisioned in Ref. [4]—have instead eluded experimental realization so far.

A Bose-Bose mixture is particularly suitable to associate such dimers due to the high phase-space densities achievable, while the atom-dimer relaxation, which limits the lifetime of the molecules, can be strongly suppressed in optical lattices with a single atom pair per lattice site [12]. A few double-species Bose-Bose mixtures have shown Feshbach resonances—e.g., ^{7}Li^{87}Rb [13] and ^{87}Rb^{133}Cs [14]—but to date double BECs have been obtained only with ^{41}K^{87}Rb [15,16]. The recent breakthrough achievement of an ultracold molecular sample in the rovibrational ground state [17] makes the Bose-Bose ^{41}K^{87}Rb mixture truly promising for the experimental observation of BECs of dipolar molecules. Following a different route, other experiments have obtained ultracold heterospecies Fermi-Fermi mixtures [18,19] that also can provide a way to compound bosonic dimers.

Here, we report on the production of heterospecies ^{41}K^{87}Rb bosonic molecules starting from an ultracold mixture. In proximity of Feshbach resonances (FRs) at moderate magnetic fields, by adding a modulation to the Feshbach field [20], we have converted up to 12 000 ^{41}K^{87}Rb pairs into dimers—i.e., 40% of the minority ^{41}K atoms—at temperatures between 200 and 600 nK. We measure the molecular lifetime to exceed 60 μs at atomic densities of $\sim 5 \times 10^{11}$ cm^{-3} for each species.

As described earlier [16], we start from a double-species magneto-optical trap (MOT) of ^{41}K and ^{87}Rb loaded by two separate two-dimensional (2D) MOTs. A quadrupole magnetostatic trap moves the atoms to the center of a millimetric Ioffe trap, which confines the sample during microwave evaporation on the ^{87}Rb hyperfine transition and allows for sympathetic cooling between Rb and K. At a temperature of 1.5 μK, we load an optical trap created by two orthogonal laser beams ($\lambda = 1064$ nm, waist$=110$ μm) and transfer ^{87}Rb and ^{41}K from the $|F=2, m=2\rangle$ to the $|1, 1\rangle$ state by microwave and radio-frequency (rf) adiabatic passage, respectively, in the presence of a 7-G bias magnetic field. All ^{87}Rb atoms left in $|2, 2\rangle$ ($\sim 10\%$) are removed by a pulse of resonant light. No blast light is needed for ^{41}K atoms. At this stage we turn on a uniform magnetic Feshbach field of approximately 78 G, close to the previously observed FR [16], corresponding to a value of the interspecies scattering length $a \sim 200 a_0$. By lowering the dipole trap power, we further evaporate the gas down to a temperature as low as 200 nK. At this temperature we have approximately $4(3) \times 10^4$ atoms of ^{87}Rb (^{41}K).

To associate KRb molecules we bring the Feshbach field to the desired value below the resonance position B_0 and modulate it by adding a rf field of typical amplitude ~ 130 mG, as depicted in Fig. 1(a). This modulation pulse has a simple square envelope, with a typical duration of 20 ms. At magnetic fields B lower than the resonance value B_0, dimers are created when the modulation frequency f_m is close to the binding energy E_b/h of the molecular level. The production of molecules is revealed by the reduction of the total number of atoms $N = N_K + N_{Rb}$ at the end of the rf pulse, as we scan the modulation frequency. A typical line shape representing the molecular association peak is reported in Fig. 1(b). Our molecules decay, most likely because of

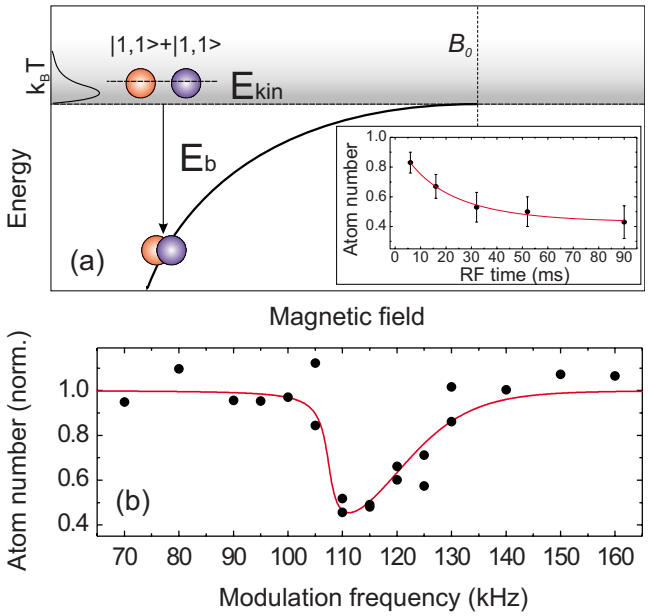

FIG. 1. (Color online) (a) Molecular radio-frequency association: two free atoms with relative kinetic energy E_{kin} are resonantly transferred to a molecular level by modulating the magnetic field. The inset shows the remaining atom number after a variable association time. The solid line is an nonexponential fit to data (see text). (b) Spectrum for an association time of 30 ms, B=78.25 G. The solid line is a fit with the line shape described in the text.

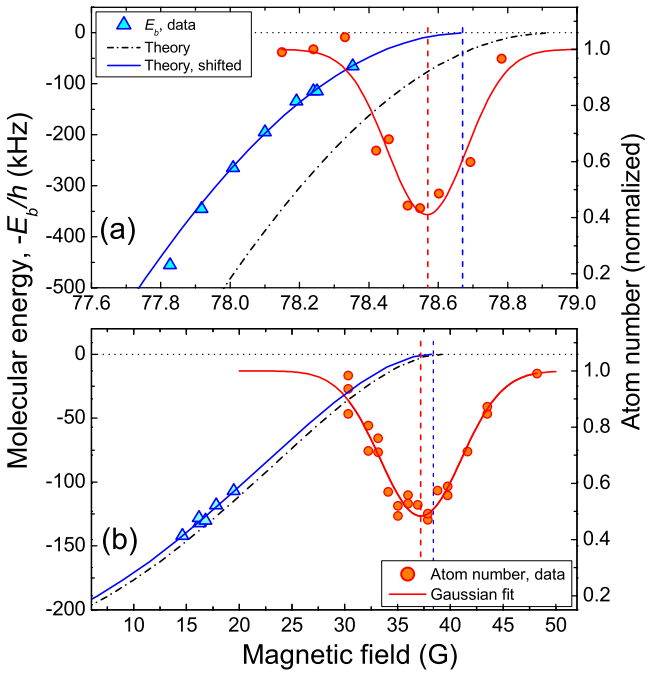

FIG. 2. (Color online) (a) KRb binding energy and three-body losses for the Feshbach resonance at 79 G: triangles show the experimental binding energies, circles the atom number. The dash-dotted black line shows the theoretical prediction for E_b; the solid blue line is the same curve, but translated by −0.24G. The solid red line represents a Gaussian fit to the atom number. The vertical dashed lines show the position of the FR as determined by the three-body losses (red, left) and the binding energy (blue, right). (b) Same as above, for the FR at 39 G. Note the widely different scale of x axis. Here the theoretical model for E_b is shifted by −1G.

vibrational quenching induced by collisions with unpaired atoms [9], and leave the trap releasing the acquired binding energy. In the absence of direct imaging of the molecules, the rf association resonance provides a clear signature of molecule production, which, in turn, can be masked by inelastic atom losses with a magnetic field sweep across the FR. In addition, rf association provides a useful characterization of the molecular spectrum.

For several values of B, we measure the corresponding binding energy by fitting the experimental rf spectra with the line shape model described later: the results are shown in Fig. 2 together with the theoretical predictions of the collisional model [21]. For both FRs the agreement is fairly good, provided the theoretical curve is translated by −0.24 G [Fig. 2(a)] and −1 G [Fig. 2(b)] along the B-field axis. A precise determination of the position of the FRs is given by the points where the molecular energy curves fitting our data cross the E_b=0 threshold: 38.4 G and 78.67 G. To stress the sensitivity of this method, it is worth remarking that a deviation of 50 mG in the B field leads to a shift of ~50 kHz in the binding energy of the leftmost experimental point of Fig. 2(a). In our experiment, the Feshbach-field stability represents the main limitation on the precision of this method. We calibrate the Feshbach field from the frequency of Rb hyperfine transitions. Given the fluctuations observed during a single measurement and day to day, we associate an uncertainty of ±30 mG to the B-field values.

We compare these FR positions with the determination obtained by the three-body losses. We have repeated the loss measurements of Ref. [16]; the data are also shown in Fig. 2. For both FRs, the peak of the three-body losses lies slightly below the B value obtained by the binding energy measurements—i.e., at 37.2(2) G and 78.57(2) G. We find that these values, intermediate from those of Ref. [16] and those obtained by the binding energies, depend on the temperature and the trap depth. We conclude that a comprehensive analysis of the dynamics associated with three-body losses is required to reliably extract the FR position, especially for the the low-field broad FR. We also recall that the extrapolation to zero binding energy is performed under the assumption that the theoretical predictions of Ref. [21] are accurate except for a small shift in the B field.

Our experimental rf spectra display several interesting and nontrivial features: (i) an evident asymmetry and a pronounced broadening related to the finite temperature of the atoms, (ii) a shift of the resonant modulation frequency that increases with the modulation amplitude, and (iii) additional association peaks at fractional frequencies of the binding energy. A precise description of the above-mentioned features is crucial to accurately determine the binding energies from the measured rf spectra.

The physical reason for the asymmetric line shapes shown in Fig. 1(b) is easily understood: as discussed later, the resonant modulation frequency of a given atom pair depends on the pair kinetic energy E_{kin}; therefore, the spectrum is

inhomogeneously broadened by the asymmetric Boltzmann distribution of kinetic energies $\sqrt{E_{\rm kin}}\exp(-E_{\rm kin}/k_BT)$ [22]. Indeed, for our typical temperatures—that is, 200–600 nK—thermal broadening is the dominating contribution to the observed linewidth. The asymmetry went unobserved in related experiments of molecular association [9,20] that employ degenerate or nearly degenerate gases.

In the following we describe the simple model developed to analyze our data by combining ideas from theoretical works on photoassociation [23] and molecule association in a harmonic potential [24]. Our model is based on several simplifying assumptions. In the center-of-mass frame, we restrict ourselves to three quantum levels: one for each atomic species in the continuum and another one for the molecular bound state. Similar to [22] the multitude of continuum states is taken into account by the thermal average of the results. We start with a set of nonlinear differential equations for the amplitudes a_j $(j=1,2)$ and m of the two atomic and molecular states, respectively:

$$i\dot{a}_j = \Omega\cos(2\pi f_m t)a_k^* m, \quad k \neq j,$$

$$i\dot{m} = \Omega\cos(2\pi f_m t)a_1 a_2 - [E(t)/\hbar + i\gamma/2]m. \tag{1}$$

Here $E(t)=E_{\rm kin}+E_b(t)$; $E_{\rm kin}$ is the relative kinetic energy of the atoms in their center-of-mass frame and $E_b(t)=\eta[\Delta B + B_m\sin(2\pi f_m t)]^2$ the time-dependent binding energy at an average detuning ΔB from the FR. We use the quadratic form of E_b, with curvature η, valid in the universal regime, and include the time variation due to the modulation of the magnetic field. For reasons of simplicity, we assume that the coupling strength Ω, proportional to the modulation amplitude B_m, is the same for all states under consideration and that the molecule decay rate γ is independent of atomic and molecular densities. We verified that, in our simplified model, we can account for inhomogeneous densities and partial interspecies overlap by rescaling the coupling strength.

Numerical solutions of Eq. (1) describe several key features of our experimental observations: For sufficiently small modulation amplitudes this model predicts atom loss when the modulation frequency equals $f_0 \equiv (E_{\rm kin}+E_b)/h$. The total atom number $N(t)=|a_1(t)|^2+|a_2(t)|^2$ decays nonexponentially: for balanced atomic populations, we find

$$N(f,t) = \frac{N(0)}{1+N(0)\kappa(f_m)t} \tag{2}$$

in the limit $\Omega \ll \gamma$. In our measurements we observe such a nonexponential decay, as shown in the inset of Fig. 1. This corresponds to the solution of the rate equation $\dot{N}=-\kappa(f_m)N^2$, which is characteristic of a two-body process. The calculated atom loss coefficient $\kappa(f_m)$ shows a Lorentzian dependence on the modulation frequency f_m, with center and width given by f_0 and γ. In order to account for the thermal distribution of the kinetic energies, we still fit our spectra with Eq. (2), but replace $\kappa(f_m)$ by its convolution with the Boltzmann distribution: the results well describe our data, as shown in Fig. 3.

Together with the binding energy, from fits we obtain an estimate for the molecular lifetime $\tau=1/\gamma=60$ μs with an uncertainty of a factor of 3. For comparison we report in Fig. 3 also the fit assuming no decay: it is evident that the finite γ smoothens the left edge of the line shape. Actually, from the spectra we can only infer a lower limit for the lifetime—that is, $\tau>20$ μs—while an upper limit of $\tau<5$ ms is instead deduced from the lack of an observable atom decay after the rf pulse is terminated. However, since unitarity constrains the inelastic atom-dimer collisions to give a lower limit for the lifetime of the order of 100 μs, we believe that the observed smoothening is likely due to technical reasons—e.g., magnetic field fluctuations.

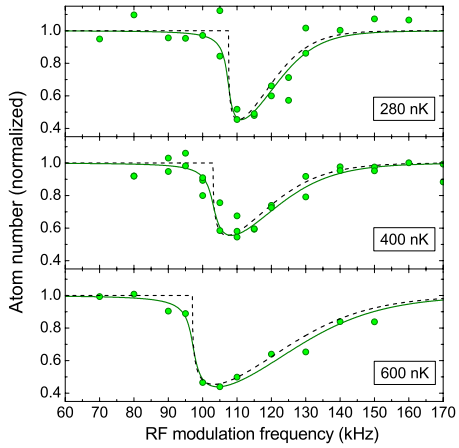

FIG. 3. (Color online) Line shapes of the molecular association process for different values of temperature. Solid circles represent data, taken after 30 ms of rf pulse length around $B=78.2$ G. Solid lines represent the fitted line shape with the model described in the text: we take the binding energy E_b, the decay rate γ, and the coupling strength Ω as free fit parameters. The temperature is measured from the ballistic expansion of the clouds. Dashed lines show the fits assuming $\gamma=0$.

As mentioned above, other nontrivial features appear at high modulation amplitudes, which are also described by our model. First, we observe a shift of the modulation resonant frequency, increasing with the modulation amplitude (see Fig. 4), which can be understood in a very direct way considering the quadratic dependence of the binding energy on the magnetic field: the time-averaged value of the transition energy $\langle E(t)\rangle$ in Eq. (1) deviates from the value $E_{\rm kin}+\eta\Delta B^2$

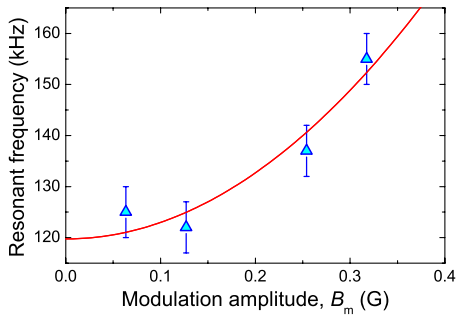

FIG. 4. (Color online) Shift of the resonant modulation frequency as a function of the modulation amplitude, measured at $B=78.30$ G with 15 ms of rf pulse length and a temperature of 350 nK. The solid line represents the parabolic fit.

by an amount $\eta B_m^2/2$. We directly verified this result by measuring the resonant modulation frequency as a function of the modulation amplitude B_m (see Fig. 4). As a consequence, for the high-field FR we extrapolate to zero modulation amplitude and correct the measured resonant frequencies by −6 kHz, corresponding to our modulation amplitude of 0.13 G. For the low-field FR, no shift due to the amplitude modulation occurs since the molecular level is approximately linear with the magnetic field.

Moreover, we observe additional loss peaks occurring when the modulation frequency is at fractional values of the average transition energy $hf_m = \langle E(t) \rangle / n$ with integer n. This allows us to access a range of binding energies which lie outside the usable bandwidth of our excitation coil. The data points at large binding energy of Fig. 2 are deduced from such measurements with a modulation frequency corresponding to half the transition energy.

Finally, we comment on the markedly different association efficiency observed between the two FRs. On the low-field Feshbach resonance the dimers' association shows a much poorer efficiency and requires an rf pulse of 1 s at maximum modulation amplitude 0.5 G. This can be understood considering that the coupling strength Ω of Eq. (1) is significant only at field detunings ΔB where the bare states of the open and closed channels mix and the energy of the molecular level deviates from the linear dependence on the B field [25]. As shown in Fig. 2, this is clearly the case only for the Feshbach resonance around 79 G. Indeed we calculate that, in the range of our measurements, Ω is approximately a factor of 10 smaller on the low-field FR, also taking into account the larger modulation amplitude employed. The reduction of the association rate by two orders of magnitude is reflected in the need for an elongated rf pulse.

In conclusion, we have reported the creation of heteronuclear $^{41}K^{87}Rb$ ultracold molecules, representing the first feasible starting point toward a BEC of dipolar molecules, since the different electronic structure of the constituents allows for a permanent electric-dipole moment in the rovibrational ground state. On the most favorable FR, with thermal clouds at 200 nK we converted up to 40% of the minority atoms. We carried out a detailed yet simple analysis of the association, highlighting a remarkable shift of the atom-molecule transition that must be taken into account for a proper determination of the binding energy, when the latter depends nonlinearly on the Feshbach field.

We plan to confine the atoms in an optical lattice [26] to suppress the molecular decay due to inelastic collisions. This should grant enough time to drive the molecules to a lower—possibly the ground—vibrational state [17,27]. Last but not least, molecular association will also serve as an important tool in the exploration of the quantum phases of the Bose-Bose mixture in the optical lattice, made possible by tuning the interspecies interactions [16]. Recently, we have become aware of the production of bosonic molecules from the Fermi-Fermi mixture $^6Li^{40}K$ [28].

This work was supported by CNR (EuroQUAM-QUDIPMOL), Ente CdR Firenze, EU (STREP NAME-QUAM, CHIMONO), and INFN (SQUAT-Super). We thank G. Varoquaux, A. Simoni, F. Ferlaino, and our colleagues of the Quantum Degenerate Gases group at LENS for fruitful discussions.

[1] K. Goral, L. Santos, and M. Lewenstein, Phys. Rev. Lett. **88**, 170406 (2002).
[2] D. DeMille, Phys. Rev. Lett. **88**, 067901 (2002).
[3] A. Micheli, G. K. Brennen, and P. Zoller, Nat. Phys. **2**, 341 (2006).
[4] L. Santos, G. V. Shlyapnikov, P. Zoller, and M. Lewenstein, Phys. Rev. Lett. **85**, 1791 (2000).
[5] M. G. Kozlov and L. N. Labzowsky, J. Phys. B **28**, 1933 (1995).
[6] R. H. Wynar *et al.*, Science **287**, 1016 (2000).
[7] E. A. Donley *et al.*, Nature (London) **417**, 529 (2002); F. A. van Abeelen and B. J. Verhaar, Phys. Rev. Lett. **83**, 1550 (1999); F. H. Mies, E. Tiesinga, and P. S. Julienne, Phys. Rev. A **61**, 022721 (2000).
[8] C. Ospelkaus *et al.*, Phys. Rev. Lett. **97**, 120402 (2006).
[9] J. J. Zirbel *et al.*, Phys. Rev. Lett. **100**, 143201 (2008); J. J. Zirbel *et al.*, Phys. Rev. A **78**, 013416 (2008).
[10] C. Klempt *et al.*, e-print arXiv:0809.0340v1.
[11] S. B. Papp and C. E. Wieman, Phys. Rev. Lett. **97**, 180404 (2006).
[12] G. Thalhammer *et al.*, Phys. Rev. Lett. **96**, 050402 (2006).
[13] C. Marzok *et al.*, e-print arXiv:0808.3967v1.
[14] F. Ferlaino (private communication).
[15] G. Modugno, M. Modugno, F. Riboli, G. Roati, and M. Inguscio, Phys. Rev. Lett. **89**, 190404 (2002).
[16] G. Thalhammer *et al.*, Phys. Rev. Lett. **100**, 210402 (2008).
[17] K.-K. Ni *et al.*, e-print arXiv:0808.2963v2.
[18] E. Wille *et al.*, Phys. Rev. Lett. **100**, 053201 (2008).
[19] M. Taglieber A. C. Voigt, T. Aoki, T. W. Hansch, and K. Dieckmann, Phys. Rev. Lett. **100**, 010401 (2008).
[20] S. T. Thompson, E. Hodby, and C. E. Wieman, Phys. Rev. Lett. **95**, 190404 (2005).
[21] A. Simoni *et al.*, Phys. Rev. A **77**, 052705 (2008).
[22] T. M. Hanna, T. Köhler, and K. Burnett, Phys. Rev. A **75**, 013606 (2007).
[23] M. Mackie, R. Kowalski, and J. Javanainen, Phys. Rev. Lett. **84**, 3803 (2000).
[24] J. F. Bertelsen and K. Mölmer, Phys. Rev. A **76**, 043615 (2007).
[25] T. Köhler, K. Góral, and P. S. Julienne, Rev. Mod. Phys. **78**, 1311 (2006).
[26] J. Catani, L. DeSarlo, G. Barontini, F. Minardi, and M. Inguscio, Phys. Rev. A **77**, 011603(R) (2008).
[27] F. Lang *et al.*, e-print arXiv:0809.0061v2.
[28] A.-C. Voigt *et al.*, e-print arXiv:0810.1306v1.